Cerebral Cortex March 2009;19:697–702
doi:10.1093/cercor/bhn118
Advance Access publication July 24, 2008

Dendritic Spine Morphology Determines Membrane-Associated Protein Exchange between Dendritic Shafts and Spine Heads

Sylvain Hugel[1,2,5], Mathias Abegg[1,6], Vincenzo de Paola[3], Pico Caroni[4], Beat H. Gähwiler[1] and R. Anne McKinney[1,2]

[1]Brain Research Institute, Winterthurerstrasse 190, CH-8057 Zurich, Switzerland, [2]Pharmacology and Therapeutics, 3655 Promenade Sir-William-Osler, Montréal, Quebec H3G 1Y6, Canada, [3]Cold Spring Harbor Laboratory, HHM1, New York, NY 11724, USA and [4]Friedrich Miescher Institut, Maulbeerstrasse 66, CH-4058 Basel, Switzerland

[5]Present address: INCI, UMR7168/LC2 CNRS-Université Louis Pasteur, 21 rue Descartes, 67084 Strasbourg cedex, France.

[6]Present address: Human Vision and Eye Movement Laboratory, University of British Columbia, 2550 Willow Street, Vancouver, British Columbia, Canada.

The purpose of this study was to examine whether variability in the shape of dendritic spines affects protein movement within the plasma membrane. Using a combination of confocal microscopy and the fluorescence loss in photobleaching technique in living hippocampal CA1 pyramidal neurons expressing membrane-linked GFP, we observed a clear correlation between spine shape parameters and the diffusion and compartmentalization of membrane-associated proteins. The kinetics of membrane-linked GFP exchange between the dendritic shaft and the spine head compartment were slower in dendritic spines with long necks and/or large heads than in those with short necks and/or small heads. Furthermore, when the spine area was reduced by eliciting epileptiform activity, the kinetics of protein exchange between the spine compartments exhibited a concomitant decrease. As synaptic plasticity is considered to involve the dynamic flux by lateral diffusion of membrane-bound proteins into and out of the synapse, our data suggest that spine shape represents an important parameter in the susceptibility of synapses to undergo plastic change.

Keywords: compartmentalization, FLIP, lateral diffusion, photobleaching, plasticity

Introduction

Dendritic spines are small protrusions consisting of a head bearing the postsynaptic components of excitatory synapses and a neck connecting the spine head to the dendritic shaft. The structure of heads and necks varies considerably among different spines within the cortex and hippocampus (Harris and Kater 1994) and over time (Fischer et al. 1998), suggesting that changes of structure entail functional consequences. It has been previously demonstrated that spine shape influences the compartmentalization of electrical signals (Tsay and Yuste 2004), calcium dynamics (Hayashi and Majewska 2005; Holcman et al. 2005; Noguchi et al. 2005) and protein synthesis (Steward and Schuman 2001) in many different neuronal systems.

The diffusion of soluble cytoplasmic proteins through the dendritic spine neck has been shown to be regulated by neuronal activity, a compartmentalization that was independent of spine shape (Bloodgood and Sabatini 2005). In cultured hippocampal neurons, a 20 times faster exchange of surface α-amino-3-hydroxy-5-methyl-4-isoxazole propionic acid (AMPA) receptors was observed in stubby spines compared with mushroom spines (Ashby et al. 2006). However, morphological parameters such as surface or length of spines, known to vary considerably among different spines (Harris and Kater 1994), were not directly deducible with the pHluorin-tagged receptor approach employed in this study (Ashby et al. 2006). It remains therefore unknown whether spine morphological parameters influence the lateral diffusion of membrane-associated proteins, a question that is of great importance with respect to synaptic membrane-associated protein trafficking during synaptic plasticity. To address this point, we studied the exchange of membrane associated proteins from dendritic shafts to spine heads with a combination of confocal microscopy, allowing the 3D reconstruction of dendritic spines, and fluorescence loss in photobleaching (FLIP) to observe membrane associated protein trafficking, in living hippocampal CA1 pyramidal neurons expressing membrane-linked green fluorescent protein (mGFP).

Materials and Methods

Transgenic Mice

Variegated mice were generated by using standard techniques. A construct was generated where the cDNA for enhanced GFP was fused to the membrane-anchoring domain (first 41 aa) of a palmitoylated mutant of MARCKS29 under the Thy1 promoter. Twenty-five distinct lines were produced, each with subtly different patterns of expression (De Paola et al. 2003). Of these, L15 mice were chosen because they had a low, but consistent, number of mGFP-labeled cells within the CA1 area of the hippocampus.

Slice Cultures

Organotypic slice cultures were used for these experiments because they provide the major advantage of exhibiting preserved tissue-specific organization of synaptic connections in an in vitro preparation suitable for imaging studies. Slices (400 μm) were prepared from the hippocampi of 6-day-old L15 mice and maintained in roller tubes for 2–4 weeks before use, as previously described (McKinney et al. 1999).

Confocal Imaging

Slice cultures were transferred to a recording chamber mounted on an upright microscope (DMLFSA, Leica Microsystems, Heidelberg, Germany) equipped with a heated (32 °C) submersion chamber where slices were continuously perfused with a solution comprising 137 mM NaCl, 2.7 mM KCl, 2.5 mM $CaCl_2$, 2 mM $MgCl_2$, 11.6 mM $NaHCO_3$, 0.4 mM NaH_2PO_4, and 5.6 mM glucose. The confocal scanhead was a Leica SP2. mGFP was imaged by using the 488 nm argon laser line, with voxel dimensions of 9 × 9 x 100–150 nm. Tertiary and some secondary dendrites of mGFP-labeled pyramidal cells were imaged using a 63× water immersion long-working distance lens (HCX APOL 63× 0.9 w U-F-I, Leica Microsystems, Heildberg, Mannheim, Germany). Additional

optical sections were taken above and below the structure of interest to register changes over time. Once the images were captured, the area of interest was cropped and further processed.

3D Reconstruction

Image stacks (3D) were deconvolved with Huygens Pro software (Scientific Volume Imaging, Hilversum, The Netherlands, supplied by Bitplane, Zurich, Switzerland) running on a Silicon Graphics Octane workstation (Mountain View, CA) using a full maximum likelihood extrapolation algorithm. Volume rendering and quantification was carried out with Imaris Surpass software (Bitplane, Zurich, Switzerland) running on a Windows 2000 workstation (Professional version, Microsoft, Redmond, WA). The same parameters were used for all time points of an experimental series.

Fluorescence Loss in Photobleaching

FLIP experiments were carried out by repeatedly bleaching the dendritic shaft with 100% of the 488-nm laser line during image frame acquisition at a frequency of 2.49 Hz during 280.7 s (line scanning frequency of 1000 Hz). Average fluorescence was measured in the spine head. Each FLIP session was preceded by acquisition of 50 frames (at 2.49 Hz) to measure the intrinsic (i.e., loss of fluorescence induced by image frame acquisition) bleaching and the maximal fluorescence. Intrinsic bleaching measured in the spine head after these 50 first frames was fitted by the following monoexponential function: $y = 0.99 + 0.048 \cdot \exp(-t/3.44)$; ($n$ = 54 spines in 16 cultures) and was always less than 5% after 400 s (n = 3; Supplementary Fig. 1). For image frame acquisition, the pinhole was completely opened (600 μm) to minimize the impact of spine movements on fluorescence measurements. The image pixel dimension was 20–30 × 20–30 nm. Loss in fluorescence during photobleaching was measured subsequently in the whole spine head with Leica LCS Lite software, fitted and statistically analyzed using Origin 5.0 software (Microcal software, Leica Microsystems, Heidelberg, Mannheim, Germany). Numbers are given as mean ± SEM.

Epileptiform Activity Protocol

Epileptiform activity was induced by blocking fast inhibitory transmission with the $GABA_A$ (gamma-aminobutyric acid) receptor antagonist bicuculline methochloride (Sigma, St. Louis, MO, 20 μM) and by extracellular electrical stimulation (every 15 s) applied via a monopolar glass stimulating electrode placed in the stratum radiatum of the CA3 hippocampal region. The induction of epileptiform activity was confirmed by recording the population burst discharge (field potentials) with extracellular glass electrodes containing 3 M NaCl placed close to the imaged cell in the stratum radiatum of the CA1 hippocampal region (Supplementary Fig. 2).

Results

FLIP Kinetic Parameters Vary between Different Spines

We used organotypic hippocampal slice cultures from variegated transgenic mice expressing enhanced GFP linked to the membrane (mGFP) in a small fraction of CA1 pyramidal neurons, allowing the visualization of their neuronal membranes (Fig. 1). In all experiments, we first imaged ≈10 μm portions of second–third order dendrites using confocal microscopy, and subsequently reconstructed the spines in 3 dimensions (Fig. 1). To compare the membrane-associated protein flux between dendritic shafts and spine heads, we used a FLIP approach, which allowed us to assess the exchange rate of fluorescent molecules between these 2 compartments.

Repetitive illumination of dendritic shafts resulted in a progressive loss of fluorescence in neighboring dendritic spines (Fig. 2). After 700 illuminations at 2.49 Hz, the fluorescence of neighboring dendritic spine heads was reduced by 70.0 ± 1.4% (n = 54 spines in 16 cultures). This decrease in spine head fluorescence is reproducible after 15 min

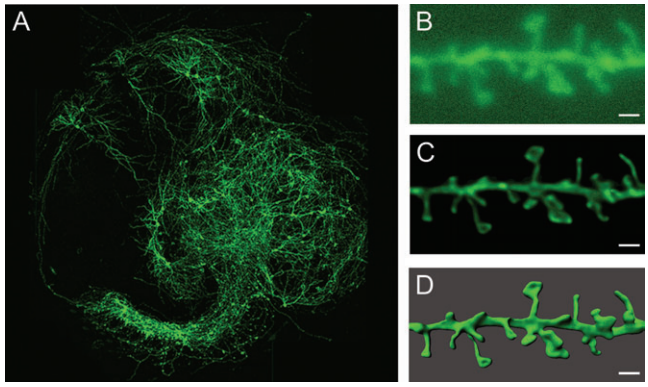

Figure 1. Hippocampal slice culture derived from variegated transgenic mouse expressing mGFP under the Thy1 promoter. (*A*) Only a subset of CA1 pyramidal neurons and dentate granule cells express mGFP in this 15-day-old hippocampal slice culture. (*B–D*) Examples of image processing prior to analysis. (*B*) maximal intensity projection of unprocessed optical slice stacks. (*C*) maximal intensity projection of the same stack after deconvolution. (*D*) Image after isosurfacing of the deconvolved data. Bar: 1 μm.

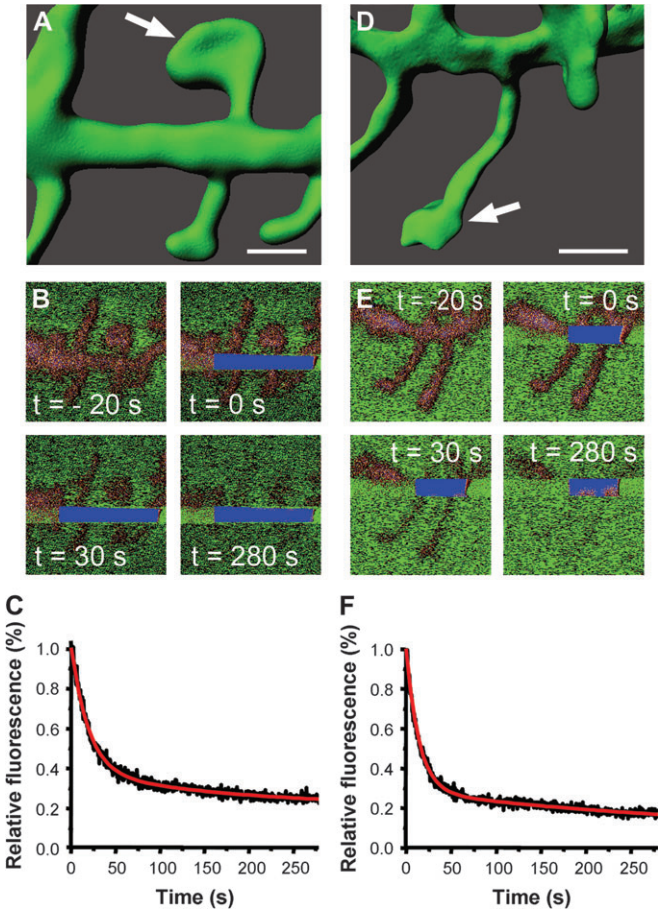

Figure 2. FLIP of a mushroom (*A–C*) and a thin (*D–F*) spine. The 3D topology of the spine is reconstructed (*A*, *D*) and the decrease in fluorescence during continuous bleaching of the dendritic shaft (*B*, *E*) is measured in the spine head. The bleached area is seen in blue, resulting from saturation of the photomultiplier. The decrease in fluorescence is best fitted by a biexponential function (*C*, *F*). Bar: 1 μm.

(Supplementary Fig. 1), and best fitted with a biexponential function: $y = y_0 + A_{fast} \cdot \exp(-x/\tau_{fast}) + A_{slow} \cdot \exp(-x/\tau_{slow})$, where in average y_0 = 30.0 ± 1.0%, corresponding to the

immobile fraction (i.e., the fluorescence that cannot be removed from the spine head compartment, whereas bleaching the parent dendritic shaft), A_{fast} = 44.3 ± 2.3%, A_{slow} = 25.3 ± 1.6%, τ_{fast} = 10.4 ± 0.64 s and τ_{slow} = 101.4 ± 13.2 s (all n = 54 spines in 16 cultures). The immobile fraction is significantly different from 0 (t-test, $P < 0.01$), indicating that a fraction of the dendritic spine membrane is not exchanged with the dendritic shaft in the time frame of the experiment. The rate of decrease in fluorescence described by the time constants (τ_{fast} and τ_{slow}) of these exponential functions corresponds to the kinetics of mGFP exchange between the dendritic shaft and the spine head compartment. FLIP kinetic parameters varied considerably between different spine shapes (Fig. 2), revealing differences in mGFP exchange between dendritic shaft and spine head compartments.

FLIP Kinetics Correlate with Dendritic Spine Shape Parameters

To assess the role of spine shape in membrane-associated protein exchange, we checked for correlations between FLIP kinetics and spine topological parameters. No correlation was detected between the immobile fraction and any of the other FLIP kinetic parameters, indicating that the size of immovable membrane pools (mostly intraspine membranes and to a small extent constrained synaptic membrane) is in this time frame not directly linked to the loss of fluorescence kinetics ($R < 0.3$ and/or $P > 0.05$, n = 54 spines).

Neither $A_{fast/slow}$ nor τ_{slow} were correlated with any of the measured spine topological parameters ($R < 0.3$ and/or $P > 0.05$, n = 54 spines for length measurements and 47 for surface measurements, in 16 cultures). Interestingly, τ_{fast}, the time constant of the fast exponential describing the decrease of 63.3% of fluorescence loss, is linearly correlated with total spine length and spine neck length (R = 0.64 and R = 0.51 respectively, $P = 1 \cdot 10^{-4}$, n = 54 spines in 16 cultures, Fig. 3). Furthermore, τ_{fast} is also linearly correlated with the total spine surface and the spine head surface (R = 0.65 and R = 0.57 respectively; $P = 1 \cdot 10^{-4}$, n = 47 spines in 16 cultures, Fig. 3). These data demonstrate the involvement of spine topological characteristics, particularly the length of spine necks and the surface of spine heads, in the exchange of mGFP from dendritic shafts to spine heads.

Epileptiform Activity-Induced Reduction in Spine Length and Surface Area is Associated with Accelerated FLIP Kinetics

On the basis of our results, we hypothesized that a reduction in length and/or volume of a given dendritic spine will be followed by an acceleration of mGFP exchange between the dendritic shaft and the spine head (and consequently by a reduction of τ_{fast}). To test this hypothesis, we took advantage of the reduction in spine length and surface occurring within minutes after induction of epileptiform activity (Supplementary Fig. 2). Epileptiform activity reduced dendritic spine length by 15 ± 6% (1.6 ± 0.1 μm vs. 1.4 ± 0.1 μm, n = 15 spines in 2 cultures, paired t-test, $P = 9 \cdot 10^{-3}$) and dendritic spine surface by 21 ± 6% (3.1 ± 0.6 μm^2 vs. 2.4 ± 0.5 μm^2, n = 12 spines in 2 cultures, paired t-test $P = 6 \cdot 10^{-3}$) (Fig. 4). As FLIP kinetics remained unchanged during successive bleaching experiments with 20 min intervals (Supplementary Fig. 1), we were able to measure FLIP kinetics before and after 30 min of epileptiform

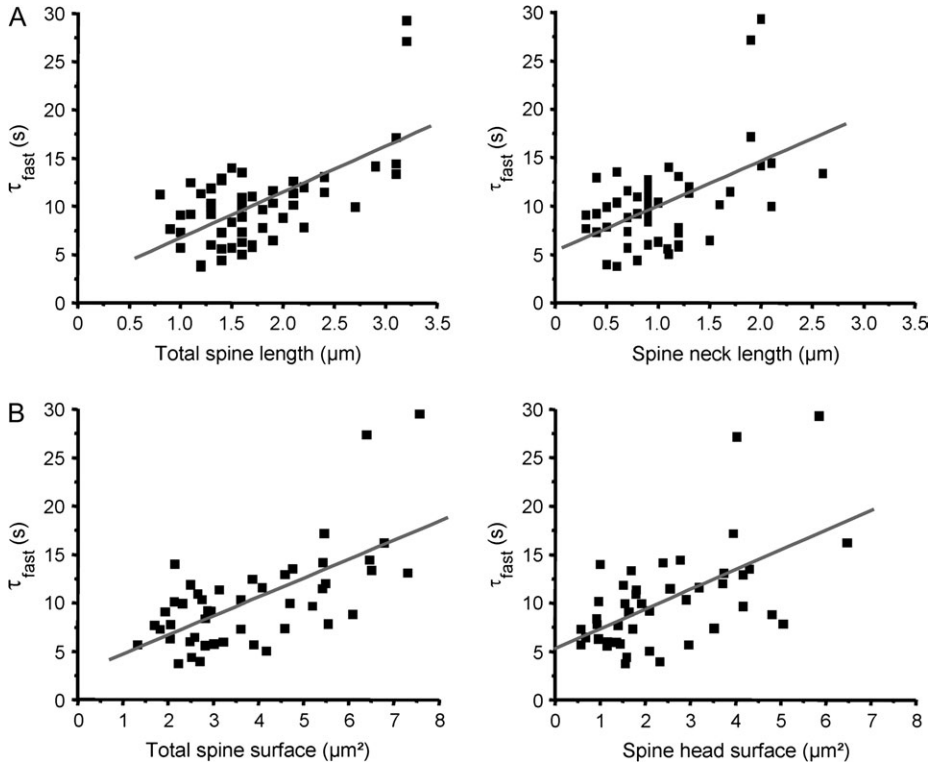

Figure 3. FLIP kinetics correlate with topological parameters of dendritic spines. (*A*) The time constant (τ_{fast}) of the faster exponential function fitting the FLIP kinetics is linearly correlated with total spine length (left) and spine neck length (right). (*B*) τ_{fast} is linearly correlated with total spine surface (left) and spine head surface (right).

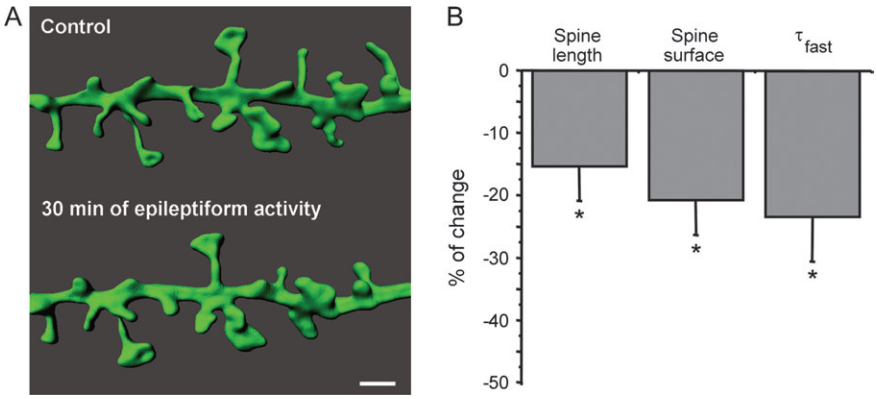

Figure 4. Epileptiform activity affects diffusion of membrane-bound molecules in spines. (*A*) Epileptiform activity reduces dendritic spine length and surface. Bar: 1 μm. (*B*) The reduction in spine length and surface induced by epileptiform activity is associated with a decrease of τ_{fast}.

activity. The reductions in dendritic spine length and surface were accompanied by a 23 ± 7% reduction of τ_{fast} (τ_{fast} control = 12.5 ± 1.4 s vs. τ_{fast} epileptiform = 9.6 ± 1.4 s, n = 12 in 2 cultures, paired t-test, P = 0.02, Fig. 4). The concomitant change of spine length/surface and τ_{fast} confirms the involvement of spine topological parameters in the control of lateral diffusion of membrane-associated molecules from dendritic shafts to spine heads.

Discussion

The present data show that neck length and head surface influence the kinetics of mGFP exchange between dendritic shaft and spine head compartments. Dendritic spines with long necks and/or voluminous heads exhibit slower membrane kinetics than those with short necks and/or small heads. To rule out the possibility that the slower kinetics in short spines are due to a difference in spine development, the spine head/dendritic shaft mGFP exchange was studied in spines that exhibited reduced length and volume as a result of epileptiform increased activity. Under these conditions, the reduction in spine neck length and head surface was clearly associated with a decrease in τ_{fast}, thus confirming the role of spine shape in the exchange of membrane-bound molecules.

As suggested by previous modeling experiments, a consequence of a spine's topology is the reduced effective surface diffusivity of membrane-bound molecules (Biess et al. 2007; Bressloff and Earnshaw 2007); this diffusion trap due to spine geometry is sufficient to account for our data.

The measured decrease in spine head fluorescence corresponds to the exchange of spine head mGFP with dendritic shaft bleached mGFP. This loss is most presumably due to lateral diffusion within the plasma membrane, as the described local recycling occurs within the dendritic spine (Brown et al. 2007) and does not involve the bleached area, and therefore cannot reduce global fluorescence of the spine head. Nevertheless, a contribution of spine head/dendritic shaft vesicle exchange in the FLIP kinetics cannot be excluded. Nevertheless, only vesicle transfer from spine head toward the shaft would result in a change in FLIP kinetics, as recycling endosome vesicles are transferred from the shaft (Brown et al. 2007) and are therefore bleached and cannot contribute to the loss of fluorescence. Such a hypothetical loss in fluorescence due to vesicle transfer from spine heads to dendritic shafts would be likely to undergo slower kinetics than lateral diffusion within the plasma membrane, and both phenomena would therefore be resolved as having distinct time constants. τ_{slow}, which is not correlated with the spine geometry, might correspond to this vesicle transfer.

We have used a GFP that is tagged to the membrane by fusion with a plasmalemmal targeting sequence modified to include palmytoylation sites (De Paola et al. 2003). At our spatial resolution, mGFP appears to uniformly stain the plasma membrane, with no detectable signal in microdomains (Supplementary Fig. 3 and also Galimberti et al. 2006). Although an artificial construct, this lipid-tethered molecule is likely to diffuse in a manner similar to endogenous freely diffusing membrane-associated molecules. This feature is particularly relevant for neurotransmitter receptors subjected to non-confined diffusion in nonsynaptic areas (Borgdorff and Choquet 2002; Dahan et al. 2003). Despite a faster diffusion of mGFP compared with AMPA receptors, both membrane-associated proteins seem to be subjected to the same constraints in dendritic spine/shaft exchange (Ashby et al. 2006). Synapses are known to be dynamic structures where membrane-associated proteins are continuously entering and leaving the synaptic scaffolding structures through lateral diffusion in the membrane leaflets (Borgdorff and Choquet 2002; Dahan et al. 2003; Ashby et al. 2004; Triller and Choquet 2005). The exchange of membrane-associated proteins between spine heads, where most excitatory postsynaptic elements are localized, and dendritic shafts, where freely diffusible neurotransmitter receptors are present at low density (Borgdorff and Choquet 2002; Dahan et al. 2003; Ashby et al. 2004; Triller and Choquet 2005; Scott et al. 2006), is therefore of fundamental importance for activity-dependent synaptic plasticity. Consequently, synaptic plastic events can be interpreted as changes in the rate of exchange of synaptic proteins such as AMPA receptors and postsynaptic density proteins such as PSD-95 between synaptic and nonsynaptic areas.

The involvement of receptor trafficking in synaptic plasticity is suggested by experiments showing that the removal of AMPA receptors from synapses during chemically induced LTD is preceded by a transient endocytosis specifically of extrasynaptic AMPA receptors (Ashby et al. 2004). Conversely, incorporation of AMPA receptors into the synapse has been demonstrated

during chemically induced long-term potentiation (LTP; Malinow and Malenka 2002), and trafficking of GluR1 from the nonsynaptic dendritic surface to the synaptic spine surface is considered to play a significant role in LTP (Bredt and Nicoll 2003). The recent demonstration of LTP-induced incorporation of AMPA receptors into synapses (Kopec et al. 2006) does not contradict this mechanism as the exact locus of exocytosis remains unknown and the diffusion of synaptic receptors subsequent to dendritic shaft exocytosis cannot be excluded.

A similar diffusion trap mechanism has also been implicated in the activity-dependent spine head recruitment of dopamine 1 receptors from dendritic shaft membrane stores (Scott et al. 2006), and the "spine geometry" diffusion trap suggested by our data might act along with the diffusion trap involving interaction with synapse scaffolding proteins (Ehlers et al. 2007) to sequester AMPA receptors in synaptic areas.

The effect of dendritic spine topology on the exchange of membrane-associated molecules between synaptic and nonsynaptic areas is likely to be a critical factor controlling the probability that a spine undergoes synaptic plasticity, as suggested by modeling studies (Biess et al. 2007). Thus, we suggest that spine shape reflects the susceptibility for plasticity rather than the state of plasticity of the synapses it bears. Our data offer an explanation for the association between plasticity and spine shape that has been observed in the hippocampus (Matsuzaki et al. 2004) and in the amygdala (Humeau et al. 2005) and for the 20 times faster turnover of AMPA receptors in short stubby spines vs. mushroom spines in cultured hippocampal neurons (Ashby et al. 2006).

Dendritic spine morphology not only varies among different spine types but also over time (Fischer et al. 1998). To assess the impact of rapid changes in spine shape, we took advantage of an epileptiform activity paradigm reducing spine length and surface within minutes. Although induced by non physiological activity, the rapid spine shape remodeling is associated with changes in the kinetics of membrane-associated exchange of molecules between spine heads/dendritic shafts, consistent with our results.

In addition to spine shape, other factors such as lipid rafts (Hering et al. 2003) and protein scaffolds can alter the lateral mobility of membrane-associated proteins. Moreover, glutamate receptor activation regulates the mobility of membrane-associated molecules in spine heads through an action on the actin cytoskeleton (Richards et al. 2004) and the trafficking of transmitter receptors (Groc et al. 2004). Together with these other mechanisms modifying lateral mobility of membrane-associated proteins between synaptic and nonsynaptic areas, rapid changes in dendritic spine shape (Fischer et al. 1998) will likely contribute to the fine-tuning of the susceptibility for plasticity of synapses located on dendritic spines.

Supplementary Material

Supplementary material can be found at: http://www.cercor.oxfordjournals.org/.

Funding

Swiss National Science Foundation Grant (31-61518.00); Canadian Institutes of Health Research operating grant to R.A.M.; Canadian Foundation of Innovation operating grant to R.A.M.; and National Sciences and Engineering Research Council of Canada operating grant to R.A.M.

Notes

We thank L. Rietschin for excellent technical assistance and Prof. U Gerber for detailed comments and critical reading of the manuscript. *Conflict of Interest*: None declared.

Address correspondence to Sylvain Hugel, PhD, Institut des Neurosciences Cellulaires et Intégratives, UMR7168/LC2 CNRS-Université Louis Pasteur, Dept. Nociception et Douleur, 1 rue René Descartes, F-67084 Strasbourg Cedex, France. Email: hugel@neurochem.u-strasbg.fr.

References

Ashby MC, De La Rue SA, Ralph GS, Uney J, Collingridge GL, Henley JM. 2004. Removal of AMPA receptors (AMPARs) from synapses is preceded by transient endocytosis of extrasynaptic AMPARs. J Neurosci. 24:5172–5176.

Ashby MC, Maier SR, Nishimune A, Henley JM. 2006. Lateral diffusion drives constitutive exchange of AMPA receptors at dendritic spines and is regulated by spine morphology. J Neurosci. 26: 7046–7055.

Biess A, Korkotian E, Holcman D. 2007. Diffusion in a dendritic spine: the role of geometry. Phys Rev E Stat Nonlin Soft Matter Phys. 76: 021922.

Bloodgood BL, Sabatini BL. 2005. Neuronal activity regulates diffusion across the neck of dendritic spines. Science. 310:866–869.

Borgdorff AJ, Choquet D. 2002. Regulation of AMPA receptor lateral movements. Nature. 417:649–653.

Bredt DS, Nicoll RA. 2003. AMPA receptor trafficking at excitatory synapses. Neuron. 40:361–379.

Bressloff PC, Earnshaw BA. 2007. Diffusion-trapping model of receptor trafficking in dendrites. Phys Rev E Stat Nonlin Soft Matter Phys. 75: 041915.

Brown TC, Correia SS, Petrok CN, Esteban JA. 2007. Functional compartmentalization of endosomal trafficking for the synaptic delivery of AMPA receptors during long-term potentiation. J Neurosci. 27:13311–13315.

Dahan M, Levi S, Luccardini C, Rostaing P, Riveau B, Triller A. 2003. Diffusion dynamics of glycine receptors revealed by single-quantum dot tracking. Science. 302:442–445.

De Paola V, Arber S, Caroni P. 2003. AMPA receptors regulate dynamic equilibrium of presynaptic terminals in mature hippocampal networks. Nat Neurosci. 6:491–500.

Ehlers MD, Heine M, Groc L, Lee MC, Choquet D. 2007. Diffusional trapping of GluR1 AMPA receptors by input-specific synaptic activity. Neuron. 54:447–460.

Fischer M, Kaech S, Knutti D, Matus A. 1998. Rapid actin-based plasticity in dendritic spines. Neuron. 20:847–854.

Galimberti I, Gogolla N, Alberi S, Santos AF, Muller D, Caroni P. 2006. Long-term rearrangements of hippocampal mossy fiber terminal connectivity in the adult regulated by experience. Neuron. 50: 749–763.

Groc L, Heine M, Cognet L, Brickley K, Stephenson FA, Lounis B, Choquet D. 2004. Differential activity-dependent regulation of the lateral mobilities of AMPA and NMDA receptors. Nat Neurosci. 7:695–696.

Harris KM, Kater SB. 1994. Dendritic spines: cellular specializations imparting both stability and flexibility to synaptic function. Annu Rev Neurosci. 17:341–371.

Hayashi Y, Majewska AK. 2005. Dendritic spine geometry: functional implication and regulation. Neuron. 46:529–532.

Hering H, Lin CC, Sheng M. 2003. Lipid rafts in the maintenance of synapses, dendritic spines, and surface AMPA receptor stability. J Neurosci. 23:3262–3271.

Holcman D, Korkotian E, Segal M. 2005. Calcium dynamics in dendritic spines, modeling and experiments. Cell Calcium. 37:467–475.

Humeau Y, Herry C, Kemp N, Shaban H, Fourcaudot E, Bissiere S, Luthi A. 2005. Dendritic spine heterogeneity determines afferent-specific Hebbian plasticity in the amygdala. Neuron. 45:119–131.

Kopec CD, Li B, Wei W, Boehm J, Malinow R. 2006. Glutamate receptor exocytosis and spine enlargement during chemically induced long-term potentiation. J Neurosci. 26:2000–2009.

Malinow R, Malenka RC. 2002. AMPA receptor trafficking and synaptic plasticity. Annu. Rev. Neurosci. 25:103–26.
Matsuzaki M, Honkura N, Ellis-Davies GC, Kasai H. 2004. Structural basis of long-term potentiation in single dendritic spines. Nature. 429: 761–766.
McKinney RA, Capogna M, Dürr R, Gähwiler BH, Thompson SM. 1999. Miniature synaptic events maintain dendritic spines via AMPA receptor activation. Nat Neurosci. 2:44–49.
Noguchi J, Matsuzaki M, Ellis-Davies GC, Kasai H. 2005. Spine-neck geometry determines NMDA receptor-dependent Ca2+ signaling in dendrites. Neuron. 46:609–622.
Richards DA, De Paola V, Caroni P, Gähwiler BH, McKinney RA. 2004. AMPA-receptor activation regulates the diffusion of a membrane marker in parallel with dendritic spine motility in the mouse hippocampus. J Physiol. 558:503–512.
Scott L, Zelenin S, Malmersjo S, Kowalewski JM, Markus EZ, Nairn AC, Greengard P, Brismar H, Aperia A. 2006. Allosteric changes of the NMDA receptor trap diffusible dopamine 1 receptors in spines. Proc Natl Acad Sci USA. 103:762–767.
Steward O, Schuman EM. 2001. Protein synthesis at synaptic sites on dendrites. Annu Rev Neurosci. 24:299–325.
Triller A, Choquet D. 2005. Surface trafficking of receptors between synaptic and extrasynaptic membranes: and yet they do move!. Trends Neurosci. 28:133–139.
Tsay D, Yuste R. 2004. On the electrical function of dendritic spines. Trends Neurosci. 27:77–83.